Supporting Information for

# Radioactive $^{198}$Au-Doped Nanostructures with Different Shapes for *in vivo* Analyses of Their Biodistribution, Tumor Uptake, and Intratumoral Distribution

Kvar C. L. Black,[†,⊥] Yucai Wang,[‡,⊥] Hannah P. Luehmann,[†] Xin Cai,[€] Wenxin Xing,[€] Bo Pang,[‡] Yongfeng Zhao,[†] Cathy S. Cutler,[§] Lihong V. Wang,[€] Yongjian Liu,[†,*] and Younan Xia[‡,*]

[†]Mallinckrodt Institute of Radiology, Washington University School of Medicine, St. Louis, Missouri 63110, United States

[‡]The Wallace H. Coulter Department of Biomedical Engineering, Georgia Institute of Technology and Emory University, Atlanta, Georgia 30332, United States

[€]Department of Biomedical Engineering, Washington University, St. Louis, Missouri 63130, United States

[§]University of Missouri Research Reactor, Columbia, Missouri 65211, United States

[⊥]These two authors contribute equally to this work

*Address correspondence to younan.xia@bme.gatech.edu; liuyo@mir.wustl.edu

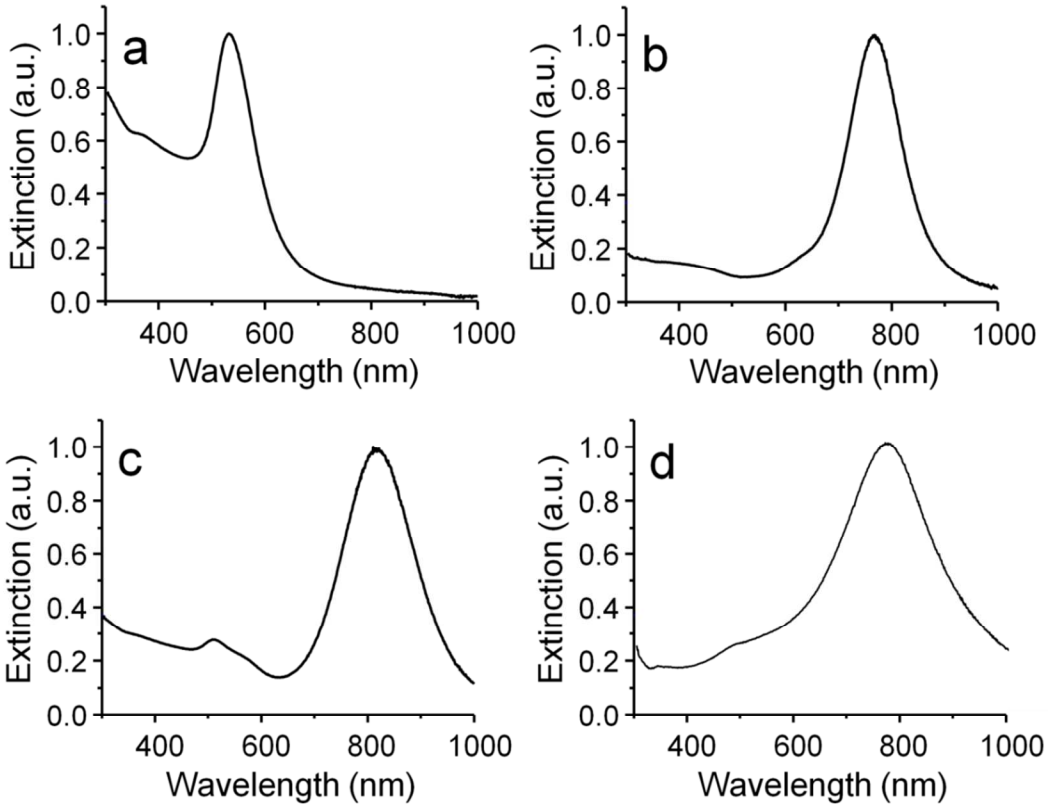


**Figure S1.** UV-vis-NIR extinction spectra of the four different types of Au nanostructures: (a) nanospheres, (b) nanodisks, (c) nanorods, (d) cubic nanocages.

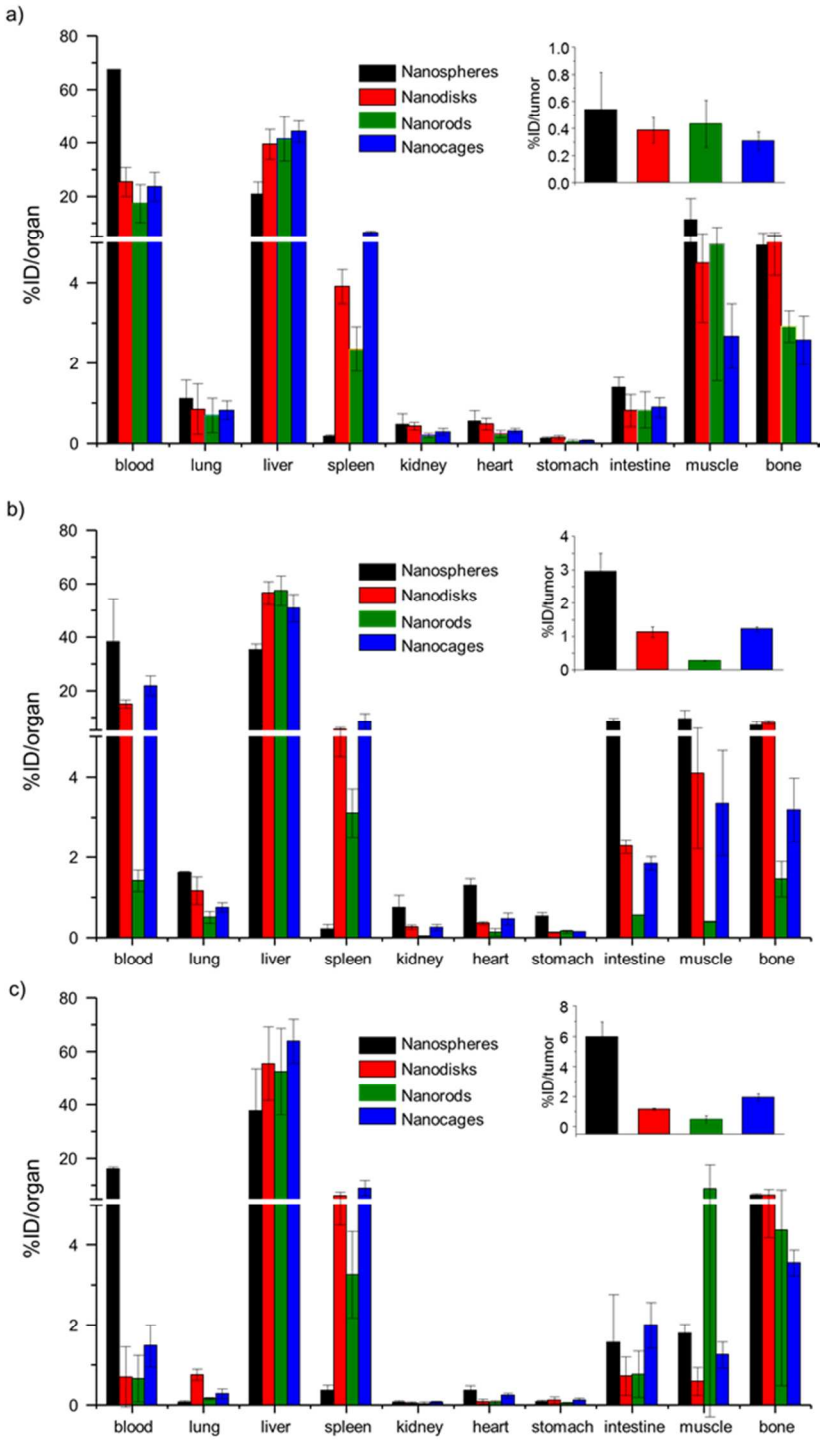


**Figure S2**. Biodistribution of the different types of $^{198}$Au-incorporated Au nanostructures at (a) 1 h, (b) 6 h, and (c) 24 h post injection. The data was presented as %ID/organ.

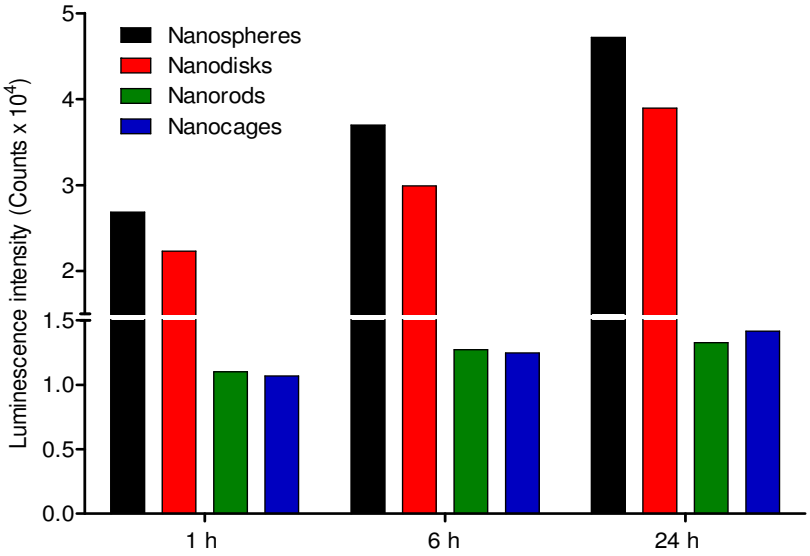


**Figure S3.** A quantitative comparison of the intensities of Cerenkov luminescence integrated from the whole tumor regions after the injection of $^{198}$Au-incorporated Au nanospheres, nanodisks, nanorods, and cubic nanocages.

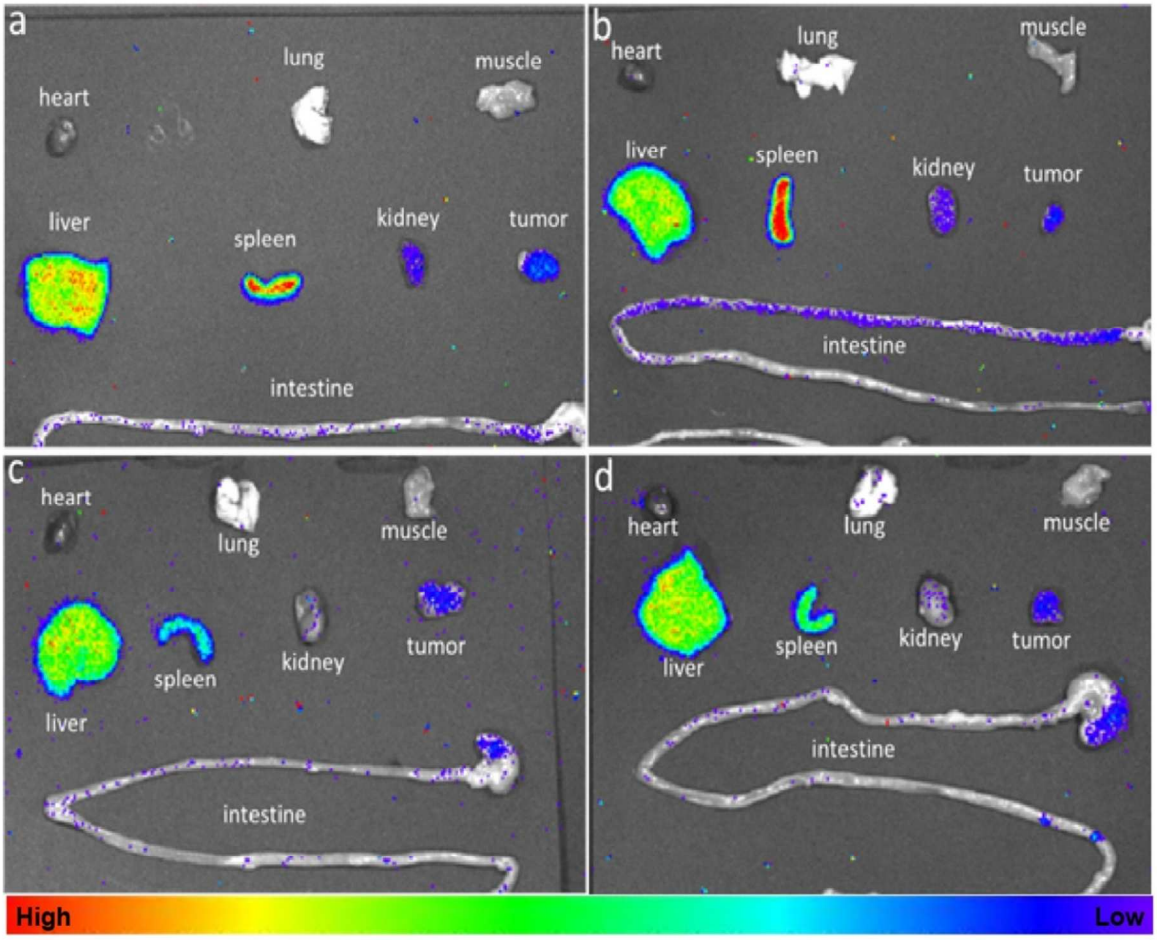


**Figure S4.** Cerenkov luminescence images of the organs that were harvested 24 h post injection of the $^{198}$Au-incorporated (a) nanospheres, (b) nanodisks, (c) nanorods, and (d) cubic nanocages. The luminescence images were merged with photographs taken using an ordinary camera.

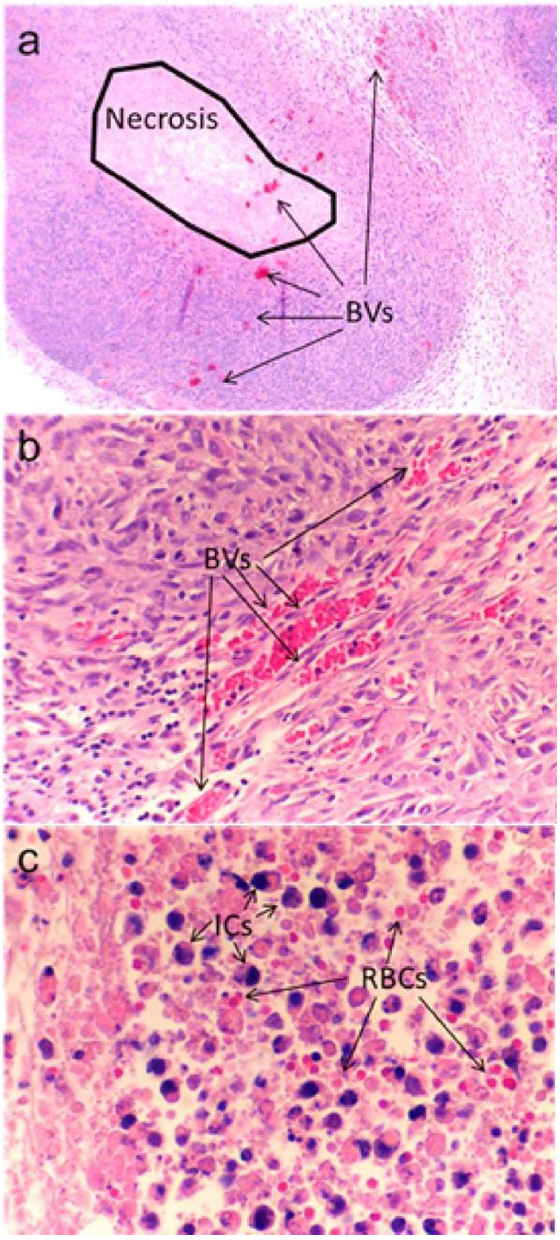


**Figure S5.** Histology of the EMT6 tumor after staining with hematoxylin and eosin (H&E). The samples show blood vessels (BVs), individual red blood cells (RBCs) from the leaky vasculature, inflammatory cells (ICs), and necrotic regions.

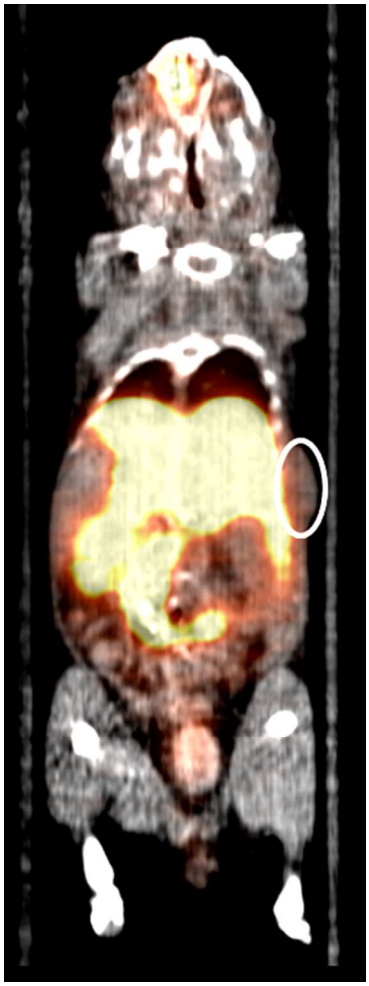

**Figure S6.** PET/CT image of a mouse bearing a EMT6 tumor (marked by the elliptic circle) after the injection of $^{64}$Cu-ATSM.

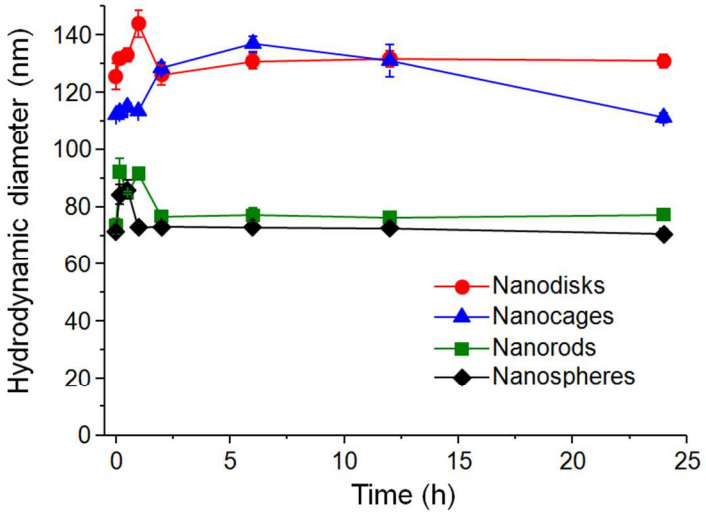


**Figure S7.** Plots of the hydrodynamic diameter of PEGylated nanostructures as a function of the incubation time. The PEGylated nanostructures were incubated with 10% Fetal Bovine Serum (FBS) in PBS at 37 ºC for different periods of time. The hydrodynamic diameter was measured using dynamic light scattering.

**Table S1.** A summary of physical parameters for the Au nanostructures used in this study.

| Nanostructures | Size (nm) | Surface area ($nm^2$) | $^{198}$Au radiolabeling specific activity (mCi/mg) |
|---|---|---|---|
| **Nanosphere** | diameter = 56.8 | 10130 | 1.6 |
| **Nanodisk** | diameter = 92<br>thickness = 7 | 13577 | 0.18 |
| **Nanorod** | length = 39.2<br>diameter = 9.1 | 1975 | 2.1 |
| **Nanocage** | edge length = 49.6<br>wall thickness = 4.5 | 14760 | 0.34 |